Proceedings of the International Conference on Industrial Engineering and Operations Management

Publisher: IEOM Society International, USA DOI: 10.46254/EU08.20250198
Published: July 2, 2025

Comparative Analysis of Machine Learning Models for Predicting Energy Consumption on Last-Mile BEV Routes

Alexandre Duarte and Hugo Tsugunobu Yoshida Yoshizaki
Department of Production Engineering
Escola Politécnica da Universidade de São Paulo
São Paulo, SP, Brazil
alexandre.duarte@usp.br, hugo@usp.br

Abstract

This article investigates the factors affecting the energy consumption of battery electric vehicles and proposes models to estimate and predict this consumption on last-mile delivery routes. First, a physical model based on GPS observations is developed to estimate energy expenditure, considering driving data (speed, acceleration, and braking), topography (road grade), transported weight, vehicle component efficiency, regenerative braking systems and use of auxiliary systems. Then, various independent variables are collected, and together with the physical model used, a hybrid approach with machine learning (ML) models is proposed to predict the energy consumption of BEVs on urban routes. A comparative analysis of the performance of different ML models is conducted. In the end, the chosen model allows for predicting energy consumption on the route based on a point-to-point energy estimation and other independent variables, providing a more reliable and accurate reference for consumption than linear parameters (kWh/km) commonly used by logistics operators.

Keywords

Battery Electric Vehicles, Energy Consumption Forecasting, Green Logistics, Machine Learning Models, Sustainable Logistics.

1. Introduction

The adoption of electric vehicles (EVs) impacts the entire supply chain, creating challenges and operational and performance difficulties for businesses, automakers, governments, and investors, who need to rethink their strategies and objectives (Alarcón et al., 2023). Due to a lack of knowledge about EV operation, users sacrifice comfort to ensure greater range, avoiding the use of air conditioning or cabin heating. Additionally, driver anxiety also affects range, such as limiting battery usage to only 50% to avoid operational risks (Anosike et al., 2021).

In the studies reviewed by Kucukoglu et al. (2021), the energy consumed by an EV is usually determined as a constant energy parameter per unit of distance (i.e., a macroscopic consumption parameter in kWh/km). However, battery consumption depends on vehicle dynamics, including speed profile, acceleration, and braking, as well as factors such as external temperature, topography, transported weight, component efficiency, and the use of auxiliary systems. This makes the use of macroscopic parameters inadequate for reliable and accurate estimates, and the variables mentioned before should be considered to achieve more realistic results in route planning (Basso et al., 2019).

Energy models for EVs allow these factors to be considered in calculating energy consumption, enabling an understanding of the influence of each one and the structuring of predictive energy consumption models. This ensures that EVs can complete their daily deliveries without the risk of running out of battery (Basso et al., 2019). The integration of energy consumption forecasting models with routing models is crucial for planning optimal and feasible routes (Macrina et al., 2019). This allows operations to be less conservative and enables the use of the electrified fleet

to its full potential (Perger and Auer, 2020). Therefore, it is essential to explore and propose methodologies to reliably predict the energy consumption of BEVs on urban routes, especially because, according to the literature review conducted by Chen et al. (2021), most studies focus on passenger vehicles, highlighting the importance of expanding the literature to include electric delivery trucks. Thus, the successful integration of BEVs into the market strongly depends on reliable energy consumption prediction models, as accurate estimation can reduce driver anxiety, improve fleet management, increase battery lifespan, optimize maintenance, and enable the identification of technical issues that affect EV performance (Ullah et al., 2022).

To develop reliable machine learning models for predicting the energy consumption of BEVs on last-mile delivery routes, one of the main challenges is obtaining real operational data with sufficient quality for model training. This study uses data collected from a distribution operation in the city of São Paulo, Brazil, contributing with a data collection and processing methodology that can be used to feed the proposed machine learning models, calibrating predictive models for different operational contexts.

This article is structured as follows: after the introduction, a literature review is presented on the most important methods and variables for predicting the energy consumption of BEVs on urban routes. In the methodology section, the hybrid approach used is described, consisting of a physics-based model that utilizes GPS data to estimate EV energy consumption and machine learning models to adjust these estimates. Next, data collection and processing of energy consumption, GPS points, and other independent variables considered are presented. This is followed by the results and discussion section, where the proposed ML models are developed and compared. Finally, the study's conclusions are presented. In the end, the aim is to understand, in a context of predicting the energy consumption of BEVs on urban delivery routes, which variables are most relevant to explaining this phenomenon, how these variables are obtained, which are the main machine learning models that can be used for the predictive task, and how each one performed. In this way, a methodology is provided that can be integrated into electric vehicle routing models, making it possible to predict energy consumption a priori, encouraging the full use of these vehicles, while avoiding cases of battery depletion in route.

2. Literature Review

2.1 Parameters that Affect the Energy Consumption of EVs

Energy consumption in EVs is influenced by a variety of parameters and factors, related to both the vehicle's components (mass, frontal area, engine power, drag coefficient, rolling resistance coefficient, battery capacity, battery temperature, SOC and SOH of the battery) and its dynamics (travel time, distance between stops, average speed, acceleration and deceleration rates), as well as traffic conditions, driving behavior, and road (gradient, distance traveled, and rolling condition) and environmental conditions (temperature, air density, wind speed, use of auxiliary systems) (Abdelaty *et al*., 2021; Chen *et al.*, 2021; Kocaarslan *et al.*, 2022).

Motor and transmission efficiency determine the percentage of energy effectively used for propulsion (Fiori *et al*., 2021), while battery state of charge (SOC) and state of health (SOH) impact energy availability and range (Peng *et al.*, 2024). Studies show that SOH declines over time, reducing operational efficiency and increasing charging frequency (Li *et al.*, 2023; Chen *et al.*, 2023). Additionally, charging methods, storage conditions, and temperature affect battery aging, with high temperatures accelerating degradation (Diwivedi *et al.*, 2024). Auxiliary systems, especially HVAC, significantly increase energy consumption, particularly at low speeds (Chen *et al.*, 2021). Rolling resistance and aerodynamic drag also play crucial roles, with road conditions, tire pressure, wind direction, and driving behavior affecting energy use (Donkers *et al*., 2020; Fiori *et al.*, 2021; Kocaarslan *et al.*, 2022). Studies highlight that poor road conditions and strong winds can drastically increase energy consumption (Abdelaty and Mohamed, 2021).

Vehicle dynamics, including factors like speed, acceleration, and braking, directly influence the energy required by EVs, and these variables are commonly used in energy estimation models (Chen *et al.*, 2021). Driver behavior also significantly impacts energy consumption, as eco-drivers, average drivers, and aggressive drivers exhibit different acceleration profiles, with aggressive driving leading to higher energy consumption, especially at high speeds (Donkers *et al.*, 2020). Additionally, changes in driving aggressiveness can significantly increase energy consumption, with variations in speed having a larger impact at speeds below 35 km/h (Abdelaty and Mohamed, 2021).

Traffic conditions, such as congestion, traffic lights, and vehicle types, significantly affect EV energy consumption (Chen *et al.*, 2021). Studies have shown that periods of heavy traffic, such as rush hour, and factors like the number

of stops per hour and congestion indexes are key variables influencing energy use (Li *et al.*, 2016; Fetene *et al.*, 2017; Xu and Wang, 2018). Environmental conditions, including road characteristics (e.g., road grade and type) and weather factors (temperature, wind, humidity), also play a crucial role (Chen *et al.*, 2021). Road inclines can dramatically increase consumption (Donkers *et al.*, 2020; Abdelaty and Mohamed, 2021), while extreme weather conditions require the use of auxiliary systems like heating and air conditioning, further raising energy use (Iora and Tribioli, 2019; Chen *et al.*, 2021). These variables should be integrated into energy consumption models for better predictions.

2.2 Energy Consumption Modeling Methodologies

Energy consumption modeling for EVs can be classified into four categories: rule-based, data-based, hybrid, and elementary models (Chen *et al.*, 2021; Dabcevic *et al.*, 2024). Elementary models consider a macroscopic parameter of constant consumption throughout the vehicle's route and are very inaccurate, given that BEV consumption is influenced by several factors, as discussed in section 2.1. Rule-based models use physical laws to estimate energy consumption, which makes it possible to incorporate the effect of various variables related to vehicle components, dynamics, traffic, driving, road surfaces and environmental conditions (Fiori *et al.*, 2021; Kocaarslan *et al.*, 2022; Pena *et al.*, 2024). However, they can be very complex and depend on accurate data collection, which can lead to estimation errors and poor real-time performance (Maity and Sarkar, 2023). Data-based machine learning models offer advantages in terms of speed and flexibility, as well as making it possible to take into account independent variables not incorporated by physical models (Dabcevic *et al.*, 2024). Nonetheless, they may lack predictability and generalization due to reliance on specific training data, which makes their predictive capacity limited when varying vehicle types, use of auxiliary systems, road characteristics, and vehicle loading (Fiori *et al.*, 2021). Hybrid models aim to combine the strengths of both approaches, improving accuracy and reducing errors (Ullah *et al.*, 2022).

Studies on EV energy consumption modeling have explored various factors affecting performance. Wang *et al.* (2017) developed an energy consumption model using GPS data and mixed-effects regression, considering road elevation and temperature but excluding speed and acceleration due to data latency. Donkers *et al.* (2020) integrated a microscopic traffic model with energy consumption prediction, accounting for traction forces and auxiliary systems. Fiori *et al.* (2021) highlighted the distinction between macroscopic and microscopic models, proposing a detailed model for instantaneous power calculation based on multiple vehicle and environmental factors. Pena *et al.* (2024) focused on energy modeling for electric garbage trucks, incorporating road profiles, exponential regenerative braking, and auxiliary systems. Other models, such as Basso *et al.* (2019) and Kocaarslan *et al.* (2022), emphasized the importance of vehicle dynamics and external factors like regenerative braking and driving behavior, while Ding *et al.* (2022) proposed a non-linear model for urban driving cycles. These studies indicate the complexity of accurately predicting EV energy consumption due to various influencing factors.

In this regard, the literature review conducted allows for the identification of a gap to be explored. Few studies propose hybrid models that use energy expenditure estimation via a physical model as an independent variable in ML models, along with other parameters that are not fully embedded in physical equations. Moreover, no study was identified in the literature that aims to perform a comparative analysis of machine learning models with an extensive set of independent variables to predict the energy consumption of BEVs on last-mile delivery routes.

This study, therefore, seeks to explore the variables described in Section 2.1, analyzing their capacity to explain battery consumption across different ML models. The following variables will be examined: distance traveled, average temperature, air humidity, distance traveled in the delivery region, total route time, weighted transported mass, terrain irregularity, wind speed, average speed, number of deliveries, rainfall, and maximum temperature. In addition, the independent variable of energy estimated by a physical model will be considered, which directly and indirectly accounts for the following aspects: vehicle mass, frontal area, battery capacity and health, motor power, accelerations, braking, distance between stops, traffic conditions, rolling surface, road grade, use of auxiliary systems, driving profile, among other factors.

A total of five ML models will be explored and compared in terms of performance: Linear Regression (LR), Artificial Neural Networks (ANN), Random Forest (RF), Support Vector Regression (SVR) and Extreme Gradient Boosting (XGB). The objective is to ultimately determine which model performed best and which independent variables are most relevant for the predictive task.

3. Methods

3.1 Physical model for energy expenditure

A microscopic physical model for point-to-point energy expenditure estimation was used (Pena *et al*., 2024). The model considers that the total energy consumption of the BEV is given by three main components (eq. 1): traction energy ($E_{traction}$), multiplied by the inverse of the overall efficiency of the BEV (eq. 2), energy for the operation of auxiliary systems (E_{aux}), and regeneration energy (E_{regen}), multiplied by the efficiency of the BEV's regenerative system (eq. 3).

The overall efficiency of the BEV, in eq. 2, takes into account the efficiencies of the motor, battery, transmission system, and converters (Donkers *et al*., 2020). The efficiency of the regenerative braking system in segment i, in eq. 3, is calculated as the product of the overall efficiency of the BEV and the exponential factor of regenerative braking in segment i ($f_{regen\,,i}$) (Peña et al., 2024).

$$E_{total} = \frac{\sum_{i=1}^{n}(E_{traction,i})}{\eta_{global}} + E_{aux} - \sum_{i=1}^{n}(E_{regen,i} \times \eta_{regen,i}) \tag{1}$$

$$\eta_{global} = \eta_{motor} \times \eta_{battery} \times \eta_{trasmission} \times \eta_{converters} \tag{2}$$

$$\eta_{regen,i} = f_{regen,i} \times \eta_{global} = \left[1 - e^{-v_i(t)}\right] \times \eta_{global} \tag{3}$$

The traction component is calculated for all segments i of the BEV's route (eq. 4) and is divided into positive kinetic energy (E_k^+), positive gravitational potential energy (E_{pg}^+), aerodynamic drag energy (E_{ad}), and rolling resistance energy (E_{rr}). The breakdown of each component can be seen in equation 5. The energy component for the operation of auxiliary systems is fixed, depending on the system's power and operating time (Basso *et al*., 2021). Finally, the regeneration energy (eq. 6) is a negative component that indicates how many kWh of the negative kinetic energy (E_k^-) were recovered during the BEV's braking phases.

$$E_{traction,i} = E_{k,i}^+ + E_{pg,i}^+ + E_{ad,i} + E_{rr,i} \tag{4}$$

$$E_{traction,i} = v_i(t)\,\Delta t_i \left[m_i\, a_i^+(t) + \frac{1}{2}\,\rho_{air}\, f_{ad}\, A_{fr}\, v_i^2(t) + m_i\, g\, \sin(\theta_i^+) + m_i\, g\, \cos(\theta)\, f_r(v_i)\right] \tag{5}$$

$$E_{regen,i} = E_k^- \times \eta_{regen,i} = v_i(t)\,\Delta t_i[m_i\, a_i^+(t)] \times \eta_{regen,i} \tag{6}$$

The variables used are defined as follows, where i denotes the segment between two subsequent GPS points: v_i is the velocity (m/s), $\Delta_{t,i}$ is the time interval (s), m_i is the total mass of the BEV (kg), $a_i(t)$ is the acceleration at instant t, p_{air} is the air density (kg/m³), g is the acceleration due to gravity (m/s²), and θ_i is the road incline. The remaining variables will be defined in the data collection section.

3.2 Energy consumption forecast model

The target variable (y) is the actual energy consumed along the route. The independent variable X_1 is the energy estimated for the route using the physical model proposed in Section 3.1. The remaining independent variables, as presented at the end of Section 2.2, are as follows: distance traveled (X_2), average temperature (X_3), air humidity (X_4), distance traveled in the delivery region (X_5), total route time (X_6), weighted transported mass (X_7), standard deviation of altitudes along the route (X_8), wind speed (X_9), average speed (X_{10}), number of deliveries (X_{11}), rainfall (X_{12}), and maximum temperature (X_{13}).

For LR, ANN, and SVR, the independent variables are selected using a forward stepwise procedure. The process begins with a model that includes only the independent variable X_1. From this initial model, additional independent variables are sequentially added, and the impact on R^2 and Mean Absolute Percentage Error (MAPE) is assessed. If the inclusion of a variable results in a significant improvement in these metrics, the variable is retained, and the next variable is evaluated. If the improvement is not substantial, the added variable is removed, and the next variable is tested. For RF and XGB, the models are developed using a backward stepwise procedure. Starting with a model that

includes all variables, an analysis of variable importance is conducted, and only those variables with an impact greater than 10% are retained.

For all models, different parameter sets were tested to improve the fit while avoiding overfitting. The parameter testing range followed recommendations from the literature (Kuhn and Johnson, 2013; Nisbet *et al*., 2009; Belyadi and Haghighat, 2021) and was expanded if the optimal parameter was found at the boundary of the interval.

For the RF, SVR, and XGBoost models, the grid search method was employed to determine the best combination of parameters. These models were provided with predefined hyperparameter ranges, and the grid search systematically tested all possible combinations to identify the optimal set that yielded the best model fit. As part of the exploratory analysis, if an optimal parameter was detected at the edge of the considered range, the interval was expanded to allow testing of additional surrounding values. Ultimately, the optimal parameter values for all models were located near the center of their respective tested ranges, indicating that the optimal region was effectively covered by the grid search process.

To validate all models, the k-fold cross-validation method was applied, ensuring that in different iterations, all data was eventually used for both training and testing. A five-fold cross-validation approach was used, with the shuffle argument set to *True*. This validation strategy enhances model robustness and generalizability, preventing overfitting to the training data and ensuring reliable performance on new, unseen data.

The analysis utilized several key Python packages, including statsmodels (v. 0.14.1), tensorflow (v.2.17.0), keras (v. 3.5.0), xgboost (v. 2.1.1), pandas (v. 2.2.0), scikit-learn (v. 1.4.1), numpy (v. 1.26.3), scipy (v. 1.12.0), seaborn (v. 0.13.2), and matplotlib (v. 3.9.1).

4. Data Collection

GPS data from electric vehicle routes were collected from a food and beverage company conducting business-to-business (B2B) deliveries in the São Paulo Metropolitan Region (RMSP), Brazil. This company operates with 42 BEVs with the characteristics described on Table 1.

Table 1. BEV characteristics.

Attribute	Value	Unit	Source
Curb weight	6380	Kg	Truck manufacturer
Payload	7920	Kg	Truck manufacturer
Battery capacity	105	kWh	Truck manufacturer
Frontal area (A_{fr})	4.45	m²	Truck manufacturer
Rolling resistance (f_r)	$f_r(v)$	-	Donkers *et al.* (2020)
Drag coefficient (f_{ad})	0.7	-	Fiori *et al.* (2021)
Motor efficiency (η_{motor})	0.95	-	Pena *et al.* (2024)
Battery efficiency ($\eta_{battery}$)	0.97	-	Pena *et al.* (2024)
Transmission efficiency ($\eta_{transmission}$)	0.96	-	Pena *et al.* (2024)
Converter efficiency ($\eta_{converters)}$	0.90	-	Pena *et al.* (2024)
Auxiliary systems (E_{aux})	1.1 $E_{traction}$	-	George and Sivraj (2021)

The proposed physical model incorporates both energy consumption for vehicle movement and auxiliary system operation. According to George and Sivraj (2021), the additional energy consumption of auxiliary systems in electric vehicles can range from 0% (best-case scenario, no auxiliary load) to 45% (worst-case scenario, all auxiliaries being used). For this model, based on George and Sivraj (2021), it was considered a 10% increase in consumption due to the constant use of electric steering. Since the use of the HVAC system is very temperature dependent, this effect will be considered on the prediction model average temperature ($\boldsymbol{X_3}$) and maximum temperature ($\boldsymbol{X_{13}}$).

Plaudis *et al*. (2021) identify two types of errors associated with GPS trajectories: measurement errors, where recorded locations differ from actual locations due to urban noise sources (Hendawi *et al*., 2020), and sampling errors, resulting

from information loss between route segments. Laranjeiro *et al*. (2019) further highlight that unrealistic speeds and accelerations can indicate erroneous GPS points. As these values are calculated using GPS positions and timestamps, they recommend applying a smoothing method before filtering out unrealistic values to remove random speed jumps that do not reflect actual behavior. Schüssler and Axhausen (2008) recommend filtering out errors corresponding to speeds exceeding 50 m/s and accelerations or decelerations exceeding 10 m/s². Therefore, the goal of data cleaning and preparation is to ensure that analyses are not influenced by errors in raw data that could distort results and lead to false analyses and misleading conclusions (Laranjeiro *et al*., 2019; Saki and Hagen, 2022).

Therefore, inspired by the structure proposed by Laranjeiro *et al.* (2019), the developed flowchart on Figure 1 describes the GPS data cleaning process. It is important to note that one step in the GPS data treatment flowchart consists of applying a map-matching algorithm. For the data collected, the Meili Valhalla map-matching service, an open-source alternative, was used. In the end, the dataset used consists of 177 observations, representing different routes carried out throughout the year 2023 in the metropolitan region of São Paulo, Brazil. The routes were completed by various vehicles from the company's fleet under study; however, all vehicles are of the same age, minimizing performance variation due to differences in vehicle lifespan.

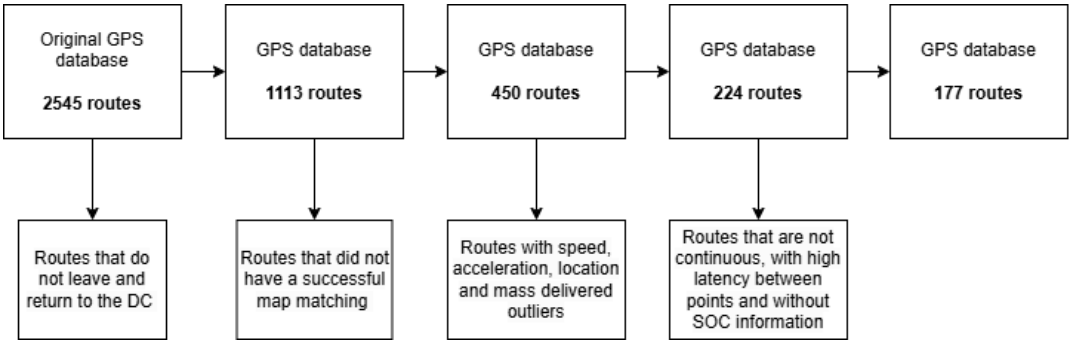

Figure 1. Data cleaning flowchart.

For the routes selected at the end of the GPS data processing flowchart, the following additional data was collected: actual energy consumption (telemetry system), total distance traveled (via map-matching service), average temperature (INMET, 2025), air humidity (INMET, 2025), distance traveled in the customer cluster (via map-matching service), total route time (GPS database), average mass transported (GPS database), standard deviation of altitudes along the route (GPS database), wind speed (INMET, 2025), average vehicle speed (GPS database), number of deliveries (GPS database), rainfall (INMET, 2025) and maximum temperature (INMET, 2025).

5. Results and Discussions

Beforehand, it is important to present the Pearson correlation matrix for the independent variables under study, which was used in the discussions below. The matrix can be viewed in Figure 2. Pearson's correlation matrix allows us to infer that the variables $\boldsymbol{X_7}$, $\boldsymbol{X_9}$, $\boldsymbol{X_{10}}$ and $\boldsymbol{X_{12}}$ are very poorly correlated with the dependent variable $\boldsymbol{y}$, which is already an indication that they will probably not be included in the final models.

In order to avoid overfitting, given the size of the sample, it's convenient to define a set of relevant $\boldsymbol{X_i}$ instead of just considering all independent variables on the models. To do so, the Pearson correlation matrix was analyzed. The variables $\boldsymbol{X_1}$ (physical estimated energy) and $\boldsymbol{X_2}$ (distance traveled) are highly correlated with the actual energy consumption ($\boldsymbol{y}$) and are thus included in this set of variables.

The variables $\boldsymbol{X_3}$, $\boldsymbol{X_4}$, $\boldsymbol{X_5}$, $\boldsymbol{X_6}$, $\boldsymbol{X_8}$, $\boldsymbol{X_{11}}$, and $\boldsymbol{X_{13}}$ are moderately correlated with the target variable. However, $\boldsymbol{X_5}$ (distance within the customer cluster) is highly correlated with $\boldsymbol{X_2}$ (distance traveled) and therefore will not be considered. The same applies to $\boldsymbol{X_6}$ (route time), which is already directly accounted for in $\boldsymbol{X_1}$, as the energy equations depend on the time interval for the route segments. The variable $\boldsymbol{X_8}$ (standard deviation of altitudes), in turn, is highly correlated with the estimated energy, given that this variability is directly included in the gravitational potential energy

component of the physical models. The variables $\boldsymbol{X_3}$ and $\boldsymbol{X_{13}}$, however, are highly correlated with each other; hence, $\boldsymbol{X_3}$ (average temperature) is retained.

Finally, the variables $\boldsymbol{X_7}$, $\boldsymbol{X_9}$, and $\boldsymbol{X_{10}}$ have low correlation with the target variable and will not be considered. The exception is the variable $\boldsymbol{X_{12}}$, which indicates the amount of rainfall. Although this variable does not show a high correlation with the target, it can serve as a proxy for identifying whether the BEV was using the HVAC system, potentially providing a better fit regarding the use or non-use of auxiliary systems.

Ultimately, the selected $\boldsymbol{X_i}$ set contains the following independent variables: $\boldsymbol{X_1}$, $\boldsymbol{X_2}$, $\boldsymbol{X_3}$, $\boldsymbol{X_4}$, $\boldsymbol{X_{11}}$, and $\boldsymbol{X_{12}}$. These variables will be used in the LR, RF, ANN, SVR, and XGB models (Figure 2).

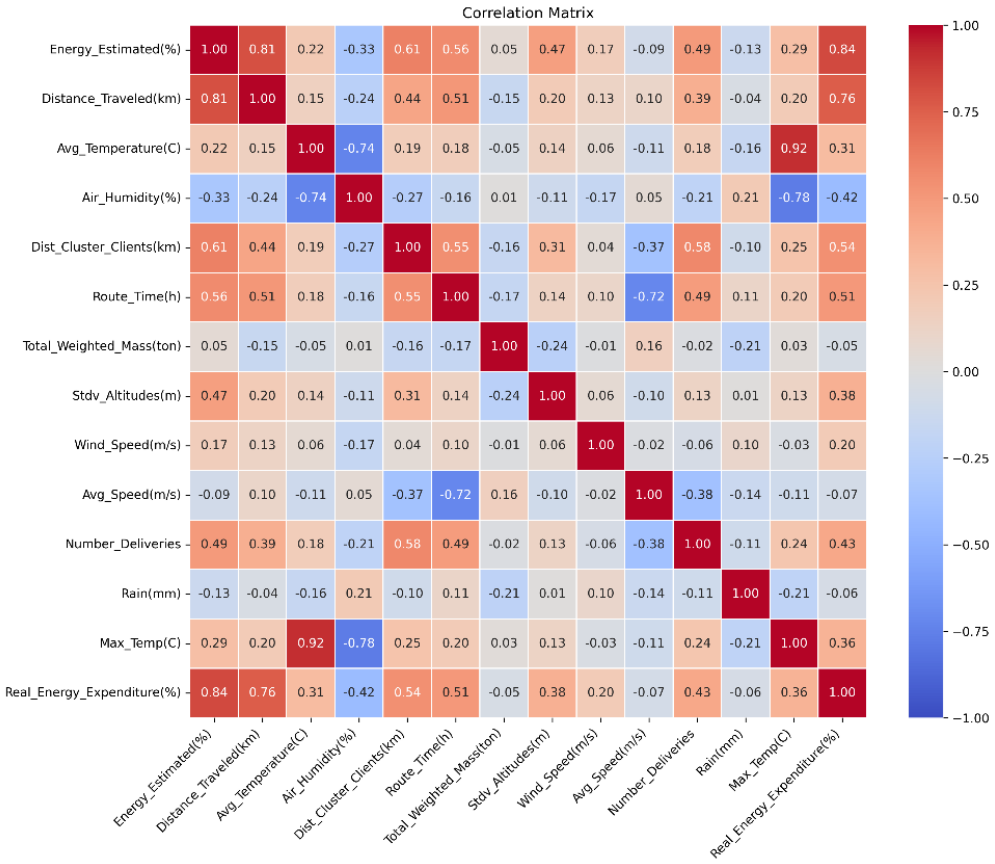

Figure 2. Pearson Correlation Matrix.

5.1 Linear Regression

Table 2 summarizes the LR results, with the intercept ($\boldsymbol{\beta}$) and $\boldsymbol{\alpha}$ coefficients associated with each of the independent variables. Variables with p-values lower than 0.01 have their coefficients marked with ***; for p-values between 0.01 and 0.05, **; for p-values between 0.05 and 0.1, *; and for p-values greater than 0.1, no marking is used, indicating that they are not statistically significant at the 90% confidence level (Fávero and Belfiore, 2017).

Table 2. LR Results.

Parameter / Model	LR
MAPE (%)	7.88
R^2	0.75
Intercept (β)	15.394**
α_1 (X_1)	0.433***
α_2 (X_2)	0.215***
α_3 (X_3)	0.150
α_4 (X_4)	-0.106**
α_{11} (X_{11})	0.023
α_{12} (X_{12})	3.033

By analyzing the p-values obtained in the initial model, it is possible to study the interactions among the independent variables. It can be observed that, following the stepwise procedure described by Fávero and Belfiore (2017), in the presence of the other independent variables, $\boldsymbol{X_3}$, $\boldsymbol{X_{11}}$, and $\boldsymbol{X_{12}}$ do not significantly contribute to explaining the phenomenon under investigation. In other words, at a 90% significance level, these independent variables are not statistically significant, and variables $\boldsymbol{X_1}$, $\boldsymbol{X_{12}}$, and $\boldsymbol{X_4}$ are sufficient to explain the behavior of the target variable.

Considering that LR is an OLS model, it is necessary to carry out some statistical tests. The model needs to have statistical significance, residuals that follow a normal distribution, homoscedastic error terms and residuals without autocorrelation (*i.e.*, independent and random). Figure 3 shows the density plot of the residuals, allowing a visual analysis of the distribution and comparison with the normal curve. Figure 3 also shows the scatter plot of the residuals, allowing us to assess whether the error terms are random and independent.

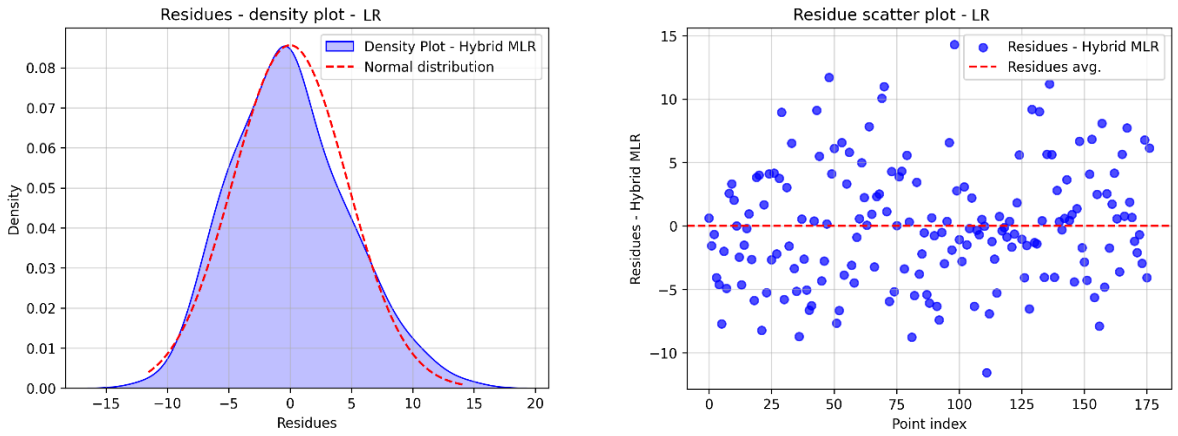

Figure 3. Residue density plot and residue scatter plot - LR.

Table 3 shows the results of the statistical tests mentioned for the LR. The model demonstrates overall statistical significance, with the F-test returning a p-value less than 0.05. Furthermore, the normality assumption of residuals was met, as the p-value of the Shapiro-Francia (SF) test is greater than 0.05, suggesting that the residuals are normally distributed. The Breusch-Pagan/Cook-Weisberg (BP/CW) test ensures that the error terms are homoscedastic. For this test, both the LM and F statistics' p-values must be greater than 0.05 for the errors to be homoscedastic at the 95% confidence level. Table 3 shows that these p-values are all greater than 0.05, confirming homoscedasticity for the model. Lastly, the Durbin-Watson (DW) test checks for autocorrelation in the residuals, ensuring they are random and independent. For this, the Durbin-Watson statistic (DW) should fall within the range [DU; 4-DU]. According to Table 3, DU < DW < 4-DU for the LR model, confirming that the residuals are random and independent at the 95% confidence level.

Table 3. LR Statistical tests results.

Parameter / Model	LR
F Test	$4.9\ x\ 10^{-51}$
SF p-value	0.155
LM p-value (BP/CW)	0.148
F p-value (BP/CW)	0.149
DW	1.893
DL	1.500
DU	1.542
4-DU	2.458

5.2 Random Forrest

For the RF, as can be seen in Table 4, the first model considers all the independent variables. In each iteration, the variable with the lowest relative importance of less than 10% is removed from the set of independent variables, and the model is compiled again. In the end, in model #4, only variables $\boldsymbol{X_1}$ and $\boldsymbol{X_2}$ remained, with relative importance of 58% and 42%, respectively. This model had a MAPE of 7.35% and an $\boldsymbol{R^2}$ of 0.76.

Table 4. RF models.

Model	MAPE	R^2	Variables and Feature Importance (X_i)
Base RF model	6.74	0.78	$X_1(50\%), X_2(26\%), X_3(9\%), X_4(8\%), X_{11}(6\%), X_{12}(0\%)$
RF #1	6.54	0.80	$X_1(44\%), X_2(32\%), X_3(10\%), X_4(7\%), X_{11}(8\%)$
RF #2	6.84	0.79	$X_1(68\%), X_2(24\%), X_3(5\%), X_{11}(3\%)$
RF #3	6.37	0.80	$X_1(68\%), X_2(27\%), X_3(5\%)$
RF #4	7.35	0.76	$X_1(58\%), X_2(42\%)$

Finally, Figure 4 shows the scatter plot of predicted y and actual y for the RF model. The support line dotted in red is given by $\boldsymbol{y_{pred} = y}$.

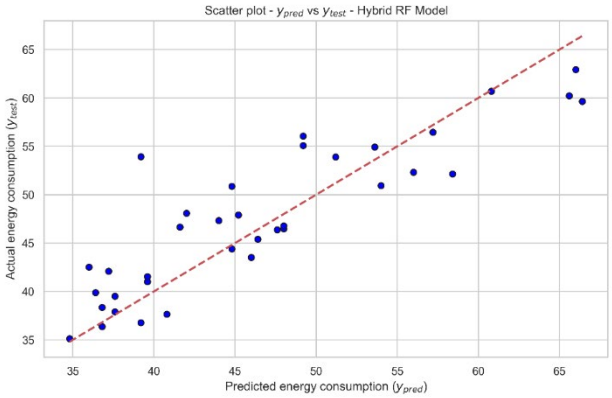

Figure 4. Predicted energy consumption vs. Actual energy consumption - RF.

5.3 Artificial Neural Network

For the ANN architecture, various configurations of layers and neurons were tested. It was observed that architectures with more than three layers did not yield substantial improvements in predictive performance. The number of neurons per layer was varied using a $\boldsymbol{2^n}$ progression; however, for $\boldsymbol{n > 7}$, no significant enhancement in fit metrics was detected. The ADAM optimizer was selected due to its robust performance across a wide range of deep learning applications. Learning rates, tested as powers of 10 starting from 0.1, showed no further improvement beyond $\boldsymbol{1 \times 10^{-5}}$. The number of epochs, representing how many times the data passes through the network, was varied in

multiples of 10. Beyond 200 epochs, no significant gains in model performance were observed. The batch size, which defines the number of training samples per iteration, was also tested using a $\mathbf{2^n}$ progression. For $\boldsymbol{n > 4}$, the model exhibited no noticeable improvement. The loss function employed was MAPE, as the objective was to minimize the mean absolute prediction error.

As can be seen on Table 5, in stage 1, the base model, which only considers variable $\boldsymbol{X_1}$ in the input layer, already has an $\boldsymbol{R^2}$ of 0.72 and a MAPE of 7.73%. In step 2, it can be seen that the only variables that help to considerably reduce the MAPE and increase the $\boldsymbol{R^2}$ are $\boldsymbol{X_2}$ and $\boldsymbol{X_3}$. In this case, $\boldsymbol{X_2}$ was added, given the greater reduction in MAPE and the greater increase in $\boldsymbol{R^2}$. In stage 3, the only variable that was added to the input layer that helped reduce the MAPE was $\boldsymbol{X_3}$. Finally, in stage 4, no added variable contributed to reducing the MAPE or increasing the $\boldsymbol{R^2}$. Therefore, in the end, model #6 was selected with 3 variables in the input layer: $\boldsymbol{X_1}$, $\boldsymbol{X_2}$ and $\boldsymbol{X_3}$, which showed an MAPE of 6.41% and an $\boldsymbol{R^2}$ of 0.82.

Table 5. ANN models.

Model	MAPE	R^2	Variables (X_i)
Base ANN model	7.73	0.72	X_1
ANN #1	7.07	0.77	X_1, X_2
ANN #2	7.10	0.73	X_1, X_3
ANN #3	8.64	0.64	X_1, X_4
ANN #4	7.72	0.70	X_1, X_{11}
ANN #5	7.97	0.71	X_1, X_{12}
ANN #6	6.41	0.82	X_1, X_2, X_3
ANN #7	7.49	0.75	X_1, X_2, X_4
ANN #8	7.10	0.81	X_1, X_2, X_{11}
ANN #9	7.22	0.77	X_1, X_2, X_{12}
ANN #10	7.18	0.72	X_1, X_2, X_3, X_4
ANN #11	6.93	0.79	X_1, X_2, X_3, X_{11}
ANN #12	7.10	0.75	X_1, X_2, X_3, X_{12}

Finally, Figure 5 shows the scatter plot of predicted y and actual y for the ANN model. The support line dotted in red is given by $\boldsymbol{y_{pred} = y}$.

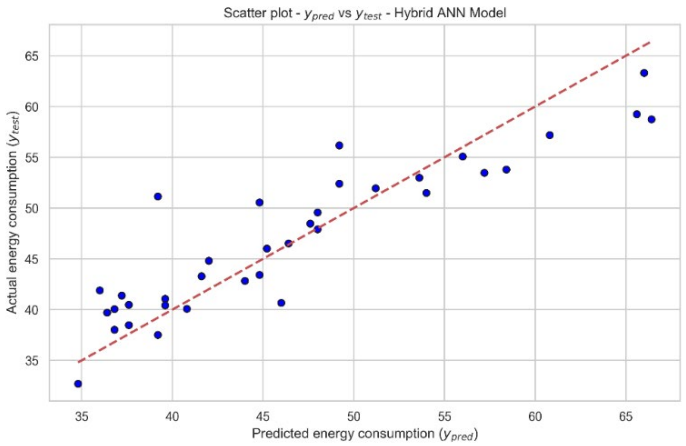

Figure 5. Predicted energy consumption vs. Actual energy consumption - ANN.

5.4 Support Vector Regression

For the SVR, as can be seen in Table 6, in stage 1, the base model, which only considers variable $\boldsymbol{X_1}$, already has an $\boldsymbol{R^2}$ of 0.74 and a MAPE of 7.28%. In step 2, it can be seen that the only variables that help to considerably reduce the

MAPE and increase the $\boldsymbol{R^2}$ are $\boldsymbol{X_2}$ and $\boldsymbol{X_4}$. In this case, $\boldsymbol{X_4}$ was added, given the greater reduction in MAPE. In stage 3, the only variable that helped reduce the MAPE was $\boldsymbol{X_2}$. Finally, in phase 4, $\boldsymbol{X_{12}}$ helped to reduce the MAPE, despite keeping $\boldsymbol{R^2}$ practically constant. So, in the end, model #12 was selected with 4 independent variables: $\boldsymbol{X_1}$, $\boldsymbol{X_2}$, $\boldsymbol{X_4}$ and $\boldsymbol{X_{12}}$, which showed a MAPE of 6.16% and an $\boldsymbol{R^2}$ of 0.81.

Table 6. SVR models.

Model	MAPE	R^2	Variables (X_i)
Base SVR model	7.28	0.74	X_1
SVR #1	6.71	0.78	X_1, X_2
SVR #2	6.94	0.74	X_1, X_3
SVR #3	6.57	0.77	X_1, X_4
SVR #4	7.54	0.73	X_1, X_{11}
SVR #5	7.59	0.73	X_1, X_{12}
SVR #6	6.53	0.82	X_1, X_4, X_2
SVR #7	6.79	0.75	X_1, X_4, X_3
SVR #8	7.00	0.76	X_1, X_4, X_{11}
SVR #9	6.77	0.77	X_1, X_4, X_{12}
SVR #10	6.45	0.81	X_1, X_4, X_2, X_3
SVR #11	6.57	0.80	X_1, X_4, X_2, X_{11}
SVR #12	6.16	0.81	X_1, X_4, X_2, X_{12}
SVR #13	6.35	0.81	$X_1, X_4, X_2, X_{12}, X_3$
SVR #14	6.74	0.80	$X_1, X_4, X_2, X_{12}, X_{11}$

Finally, Figure 6 shows the scatter plot of predicted y and actual y for the SVR model. The support line dotted in red is given by $\boldsymbol{y_{pred} = y}$.

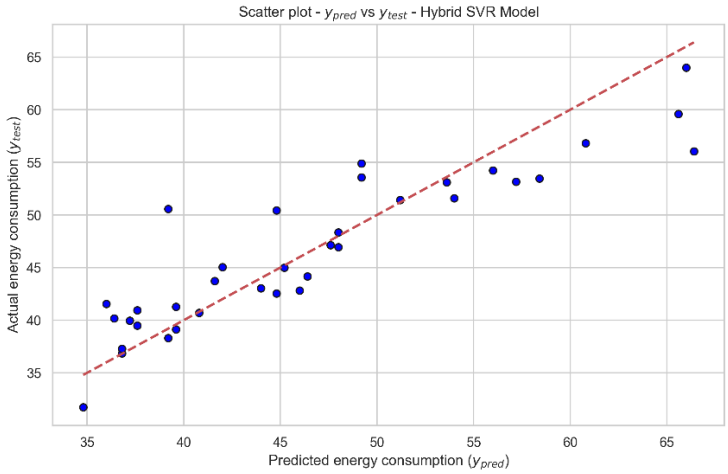

Figure 6. Predicted energy consumption vs. Actual energy consumption - SVR.

5.5 Extreme Gradient Boosting

For XGBoost, as can be seen in the Table 7, the first model considers all the independent variables. In each iteration, the variable with the lowest Relative Importance (RI), less than 10%, is removed from the set of independent variables and the model is compiled again. In the end, in model #3, only variables $\boldsymbol{X_1}$, $\boldsymbol{X_2}$ and $\boldsymbol{X_3}$ remained, with RI of 72%, 18% and 10%, respectively. However, model #2 was selected. Although $\boldsymbol{X_4}$ had a RI of 8%, model #2 had a lower MAPE and a higher $\boldsymbol{R^2}$ than model #3 (6.17% and 0.81, respectively).

Table 7. XGB models.

Model	MAPE	R^2	Variables and Feature Importance (X_i)
Base XGB model	6.96	0.80	$X_1(59\%), X_2(14\%), X_3(8\%), X_4(6\%), X_{11}(7\%), X_{12}(6\%)$
XGB #1	6.49	0.81	$X_1(53\%), X_2(23\%), X_3(9\%), X_4(9\%), X_{11}(7\%)$
XGB #2	6.17	0.81	$X_1(65\%), X_2(17\%), X_3(10\%), X_4(8\%)$
XGB #3	6.30	0.80	$X_1(72\%), X_2(18\%), X_3(10\%)$

Finally, Figure 7 shows the scatter plot of predicted y and actual y for the ANN model. The support line dotted in red is given by $\boldsymbol{y_{pred} = y}$.

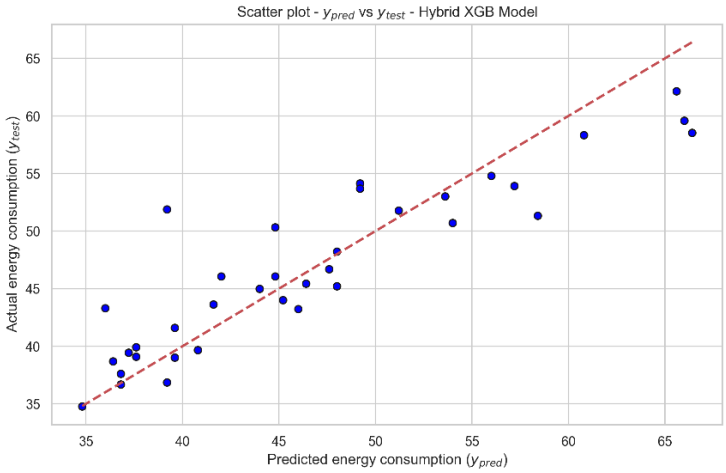

Figure 7. Predicted energy consumption vs. Actual energy consumption - XGB.

5.5 Summary of the models and discussions

Table 8 indicates the independent variables for each of the ML models. For each model, the selected $\boldsymbol{X_i}$ variables are marked with an "$\boldsymbol{x}$". Table 8 also summarizes the $\boldsymbol{R^2}$ and MAPE values for the ML models.

Table 8. Summary of the ML models.

Parameter / Model	LR	RF	ANN	SVR	XGB
MAPE (%)	7.88	7.35	6.41	6.16	6.17
R^2	0.75	0.76	0.82	0.81	0.81
$\boldsymbol{X_1}$ (Physical estimated energy)	x	x	x	x	x
$\boldsymbol{X_2}$ (Distance traveled)	x	x	x	x	x
$\boldsymbol{X_3}$ (Average temperature)			x		x
$\boldsymbol{X_4}$ (Air humidity)	x			x	x
$\boldsymbol{X_{11}}$ (Number of deliveries)					
$\boldsymbol{X_{12}}$ (Rainfall)				x	

Comparing the parameters in Table 8, it can be seen that LR and RF show clearly inferior results to the other models. ANN, SVR and XGB, on the other hand, have very similar results in terms of $\boldsymbol{R^2}$ and MAPE. To decide on the final model, the independent variables of each model are analyzed.

In the ANN, SVR and XGB models, the variables $\boldsymbol{X_1}$ and $\boldsymbol{X_2}$ were included. Only the SVR and XGB models selected the variable $\boldsymbol{X_4}$ (air humidity). The variable $\boldsymbol{X_{12}}$ (rainfall) was selected in SVR, while $\boldsymbol{X_3}$ (average temperature) was selected in ANN and XGB. In terms of ease of predicting and obtaining climate information, it was prioritized the variable $\boldsymbol{X_3}$, given that, *a priori*, temperature information is more predictable than quantitative humidity and rainfall

information in millimeters. In addition, rainfall and humidity information refers to the city as a whole, not necessarily exactly to the region where the electric vehicle is being driven. These factors combined led to the choice of the ANN model as the best one for this predictive task, *ceteris paribus*.

6. Conclusion

This study had the following general objectives: investigate the factors affecting the energy consumption of BEVs, propose models to estimate and predict this consumption, and to conduct a comparative analysis of machine learning models for predicting energy expenditure on last-mile BEV routes.

In order to achieve these objectives, a literature review was conducted to provide the theoretical basis for the methodology proposed in this work. A hybrid model was used to predict the energy consumption of BEVs on urban routes, which incorporates several aspects of vehicle dynamics through a physical estimation model and other independent variables to adjust the energy consumption using ML models. The analysis considers 13 independent variables combined in different ways.

The results obtained through the comparative analysis of the ML models allow us to conclude that a subset of the selected features is able to explain the phenomenon under study satisfactorily. LR and RF did not perform well, possibly due to LR's inability to capture non-linear relationships in the data and RF's tendency to lose precision in high-dimensional data or data with complex patterns. On the other hand, ANN, SVR and XGB outperformed, which can be explained by ANN's ability to learn complex representations, SVR's efficiency in capturing patterns in small amounts of data with well-defined edges and XGB's strength in adjusting to non-trivial relationships by boosting trees. After evaluating all ML models, the ANN was chosen, since it shows the best balance between performance (6.4% MAPE and 0.82 $\boldsymbol{R^2}$) and number of features (physically estimated energy, total distance traveled and average temperature).

This article offers a theoretical contribution to predictive energy consumption models for BEVs in the context of last-mile operations, by identifying relevant features and outlining methods to obtain the key data required to determine these features. It also contributes by comparing the performance of different machine learning models, highlighting not only the most relevant explanatory variables but also the most suitable algorithms for this specific context.

Regarding practical implications, using the models and framework proposed in this work, it is possible to predict energy consumption for electric vehicles with good statistical reliability and low error. These models can be integrated into the planning and routing stages of electric vehicle operations, supporting greener last-mile distribution with improved safety and reliability in terms of energy usage.

Some limitations of this study include the number of features used, the dataset size, and the specific operational context in which the data were collected. To develop a machine learning model with improved predictive performance outside the operational context of São Paulo, Brazil, it would be beneficial to incorporate data from BEV operations in different cities and scenarios. In this sense, future work could explore additional predictive features (e.g., vehicle's health status, it's age and driving style) and extend the methodology to other operational contexts, such as long-haul transportation, waste collection operations, and public transport. It would also be valuable to replicate the proposed method using expanded datasets that include data from operations in multiple cities, featuring diverse topographies, climates, stop densities, and other distinct operational characteristics. This would enrich both the model and the analysis by enhancing its generalizability and robustness.

References

Alarcón, F. E., Mac Cawley, A., Sauma, E., Electric mobility toward sustainable cities and road-freight logistics: A systematic review and future research directions, *Journal of Cleaner Production*, p. 138959, 2023.

Anosike, A., Loomes, H., Udokporo, C. K., Garza-Reyes, J. A, Exploring the challenges of electric vehicle adoption in final mile parcel delivery, *International Journal of Logistics Research and Applications*, v. 26, n. 6, p. 683-707, 2023.

Basso, R., Kulcsár, B., Egardt, B., Lindroth, P., Sanchez-Diaz, I., Energy consumption estimation integrated into the electric vehicle routing problem, *Transportation Research Part D: Transport and Environment*, v. 69, p. 141-167, 2019.

Basso, R., Kulcsár, B., Sanchez-Diaz, I., Electric vehicle routing problem with machine learning for energy prediction. *Transportation Research Part B: Methodological*, v. 145, p. 24-55, 2021.

Belyadi, H., Haghighat, A., Machine Learning Guide for Oil and Gas Using Python, *Gulf Professional Publishing*, 2021.

Chen, Y., Wu, G., Sun, R., Dubey, A., Laszka, A., Pugliese, P., A review and outlook of energy consumption estimation models for electric vehicles, *arXiv:2003.12873*, 2020.

Chen, J.; Chen, D.; Han, X.; Li, Z.; Zhang, W.; Lai, C. S. State-of-health estimation of lithium-ion battery based on constant voltage charging duration. *Batteries*, v. 9, n. 12, p. 565, 2023.

Dabčević, Z., Škugor, B., Cvok, I., Deur, J., A Trip-Based Data-Driven Model for Predicting Battery Energy Consumption of Electric City Buses, *Energies*, v. 17, n. 4, p. 911, 2024.

Ding, N.; Yang, J.; Han, Z.; Hao, J. Electric-Vehicle Routing Planning Based on the Law of Electric Energy Consumption. *Mathematics*, 2022.

Donkers, A., Yang, D., Viktorović, M., Influence of driving style, infrastructure, weather and traffic on electric vehicle performance. *Transportation research part D: transport and environment*, v. 88, p. 102569, 2020.

Dwivedi, S.; Akula, A.; Pecht, M. Predictive analytics for prolonging lithium-ion battery lifespan through informed storage conditions. *Energy*, v. 308, p. 133052, 2024.

Fávero, L. P.; Belfiore, P. Manual de análise de dados: estatística e modelagem multivariada com Excel®, SPSS® e Stata®, *Elsevier Brasil*, 2017.

Fiori, C., Montanino, M., Nielsen, S., Seredynski, M., Viti, F., Microscopic energy consumption modelling of electric buses: model development, calibration, and validation, *Transportation Research Part D: Transport and Environment*, v. 98, p. 102978, 2021.

Fetene, G. M.; Kaplan, S.; Mabit, S. L.; Jensen, A. F.; Prato, C. G., Harnessing big data for estimating the energy consumption and driving range of electric vehicles, *Transportation Research Part D: Transport and Environment*, Elsevier, v. 54, p. 1–11, 2017.

George, D.; Sivraj, P. Driving range estimation of electric vehicles using deep learning, *IEEE, 2021 second international conference on electronics and sustainable communication systems (ICESC),* 2021. p. 358–365.

Hendawi, A., Shen, J., Sabbineni, S. S., Song, Y., Cao, P., Zhang, Z., Krumm, J., Ali, M., Noise patterns in GPS trajectories, *21st IEEE International Conference on Mobile Data Management (MDM), IEEE*, 2020. p. 178-185.

INMET, Banco de Dados Meteorológicos do INMET, Available: https://bdmep.inmet.gov.br/, March 07, 2025.

Iora, P.; Tribioli, L. Effect of ambient temperature on electric vehicles' energy consumption and range: Model definition and sensitivity analysis based on Nissan leaf data. *World Electric Vehicle Journal, MDPI*, v. 10, n. 1, p. 2, 2019.

Kocaarslan, I., Zehir, M. A., Uzun, E., Uzun, E. C., Korkmaz, M. E., Cakiroglu, Y., High-Fidelity Electric Vehicle Energy Consumption Modelling and Investigation of Factors in Driving on Energy Consumption. *4th Global Power, Energy and Communication Conference (GPECOM)*, *IEEE*, 2022. p. 227-231.

Kucukoglu, I., Dewil, R., Cattrysse, D., The electric vehicle routing problem and its variations: A literature review, *Computers & Industrial Engineering*, v. 161, p. 107650, 2021.

Kuhn, M., Johnson, K., Applied Predictive Modeling, *Springer New York*, 2013, https://doi.org/10.1007/978-1-4614-6849-3.

Laranjeiro, P. F., Merchán, D., Godoy, L. A., Giannotti, M., Yoshizaki, H. T., Winkenbach, M., Cunha, C. B., Using GPS data to explore speed patterns and temporal fluctuations in urban logistics: The case of São Paulo, Brazil. *Journal of Transport Geography*, v. 76, p. 114-129, 2019.

Li, W.; Stanula, P.; Egede, P.; Kara, S.; Herrmann, C. Determining the main factors influencing the energy consumption of electric vehicles in the usage phase. *Procedia Cirp, Elsevier*, v. 48, p. 352–357, 2016.

Macrina, G., Pugliese, L. D. P., Guerriero, F., Laporte, G., The green mixed fleet vehicle routing problem with partial battery recharging and time windows. *Computers & Operations Research*, v. 101, p. 183-199, 2019.

Maity, A.; Sarkar, S., Data-driven probabilistic energy consumption estimation for battery electric vehicles with model uncertainty, v. 21, p. 9, *International Journal of Green Energy*, 2023.

Nisbet, R.; Elder, J.; Miner, G. D. Handbook of statistical analysis and data mining applications, *Academic press*, 2009.

Peña, D., Dorronsoro, B., Ruiz, P., Sustainable waste collection optimization using electric vehicles, *Sustainable Cities and Society*, v. 105, p. 105343, 2024.

Peng, S., Zhu, J., Wu, T., Tang, A., Kan, J., Pecht, M., SOH early prediction of Lithium-ion batteries based on voltage interval selection and features fusion, *Energy*, v. 308, p. 132993, 2024.

Perger, T., Auer, H., Energy efficient route planning for electric vehicles with special consideration of the topography and battery lifetime, *Energy Efficiency*, v. 13, n. 8, p. 1705-1726, 2020.

Plaudis, M., Azam, M., Jacoby, D., Drouin, M. A., & Coady, Y., An Algorithmic Approach to Quantifying GPS Trajectory Error, *Proceedings of the IEEE/CVF International Conference on Computer Vision*, 2021. p. 3909-3916.

Saki, S.; Hagen, T. A practical guide to an open-source map-matching approach for big gps data. *SN Computer Science*, v. 3, n. 5, p. 415, 2022.

Schüssler, N., & Axhausen, K. W., Identifying trips and activities and their characteristics from GPS raw data without further information, *Arbeitsberichte Verkehrs-und Raumplanung*, v. 502, 2008.

Ullah, I., Liu, K., Yamamoto, T., Zahid, M., Jamal, A., Prediction of electric vehicle charging duration time using ensemble machine learning algorithm and Shapley additive explanations, *International Journal of Energy Research*, v. 46, n. 11, p. 15211-15230, 2022.

Wang, J., Liu, K., & Yamamoto, T., Improving electricity consumption estimation for electric vehicles based on sparse GPS observations. *Energies*, v. 10, n. 1, p. 129, 2017.

Xu, Y., & Wang, K., Research on estimation method of mileage power consumption for electric vehicles. *International Conference on Computer Science, Electronics and Communication Engineering (CSECE 2018), Atlantis Press*, 2018. p. 504-508.

Biographies

Alexandre Duarte holds a BSc in Civil Engineering and an MSc in Logistics Systems Engineering from Polytechnic School of the University of São Paulo. He has research experience in green logistics, last-mile operations with electric vehicles and operations research. He is a researcher at the Center for Innovation in Logistics Systems at the University of São Paulo, and has participated in research and publications in the areas of urban freight logistics and humanitarian logistics.

Hugo Tsugunobu Yoshida Yoshizaki has a PhD in Industrial Engineering from Polytechnic School of the University of São Paulo. He is currently a senior professor on Logistics and Supply Chain Management in the Department of Production Engineering at the University of São Paulo, where he directs their Center for Innovation in Logistics Systems. His research interests include green logistics, urban delivery, and energy transition in logistics.